Biochemical and Biophysical Research Communications 452 (2014) 509–514

Contents lists available at ScienceDirect

Biochemical and Biophysical Research Communications

journal homepage: www.elsevier.com/locate/ybbrc

Roles of tryptophan residue and disulfide bond in the variable lid region of oxidized polyvinyl alcohol hydrolase

Yu Yang [a,1], Tzu-Ping Ko [b,1], Long Liu [a], Jianghua Li [a], Chun-Hsiang Huang [c], Jian Chen [a], Rey-Ting Guo [c,*], Guocheng Du [a,*]

[a] Key Laboratory of Industrial Biotechnology, Ministry of Education, Jiangnan University, Wuxi 214122, China
[b] Institute of Biological Chemistry, Academia Sinica, Taipei 11529, Taiwan
[c] Industrial Enzymes National Engineering Laboratory, Tianjin Institute of Industrial Biotechnology, Chinese Academy of Sciences, Tianjin 300308, China

ARTICLE INFO

Article history:
Received 18 August 2014
Available online 27 August 2014

Keywords:
p-Nitrophenyl esters
Lipase activity
Enzyme kinetics
Crystal structure
Mutagenesis

ABSTRACT

Oxidized polyvinyl alcohol hydrolase (OPH) catalyzes the cleavage of C–C bond in β-diketone. It belongs to the α/β-hydrolase family and contains a unique lid region that covers the active site. The lid is the most variable region when pOPH from *Pseudomonas* sp. VM15C and sOPH from *Sphingopyxis* sp. 113P3 are compared. The wild-type enzymes and the pOPH mutants W255A, W255Y and W255F were analyzed for lipase activity by using p-nitrophenyl (pNP) esters as the substrates. The wild-type enzymes showed increased K_m and decreased k_{cat}/K_m with the acyl chain length, and the mutants showed reduced k_{cat}/K_m for pNP acetate, indicating the importance of Trp255 in sequestering the active site from solvent. The significantly lower activity for pNP butyrate can be a result of product inhibition, as suggested by the complex crystal structures, in which butyric acid, DMSO or PEG occupied the same substrate-binding cleft. The mutant activity was retained with pNP caprylate and pNP laurate as the substrates, reflecting the amphipathic nature of the cleft. Moreover, the disulfide bond formation of Cys257/267 is important for the activity of pOPH, but it is not essential for sOPH, which has a shorter lid structure.

1. Introduction

Polyvinyl alcohol (PVA) has been widely used in the industry and may cause environmental problems. However, PVA is biodegradable by oxidation and hydrolysis. Oxidized PVA hydrolase (OPH) was identified in hydrolyzing oxidized PVA (OPA) [1,2], which is a product of PVA dehydrogenase or oxidase [3]. Previously we obtained the crystal structures of pOPH from *Pseudomonas* sp. VM15C and sOPH from *Sphingopyxis* sp. 113P3 [4]. Analyses of the crystal structures and amino-acid sequences of related proteins confirmed that OPH belongs to the α/β-hydrolase family.

The α/β-hydrolase family is constantly expanding. They are mainly involved in breaking C–O bond (as in esterase and lipase), C–N bond (protease), C–S bond (thioester hydrolase), C–C bond (β-diketone hydrolase), and so on [5]. The core of α/β-hydrolase contains a highly conserved catalytic triad [6]: a nucleophile residue (Ser or Cys), a His residue, and an acidic residue (Asp or Glu). The nucleophile residue is located in a sharp turn, so called the "nucleophile elbow", which has a consensus sequence Sm-X-Nu-X-Sm (Sm = small residue, mostly Gly, X = any residue, and Nu = nucleophile residue). The oxyanion hole is always formed by the backbone amides to stabilize the transition state during the catalytic reactions [6]. Interestingly, in our previous study, a double oxyanion hole was identified in OPH.

The two OPH structures also showed a lid region with β-ribbon topology. The lid, covering the active site, is seen in most lipases as well but is always an amphipathic helix. When lipases hydrolyze nonpolar substrates, it is essential to expose the hydrophobic binding pocket by changing the lid region from "close" form to "open" form [7]. In addition, the lid plays a key role in substrate specificity of lipases [8]. Xu et al. reported a structure of lipase from *Malassezia globosa* (SMG1; PDB 3UUE), which is strictly specific for mono- and diacylglycerol [9]. Trp229 and Phe278 were considered as key residues to hinder triacylglycerol binding. The mutants of W299L and W116A altered the substrate preference and improved the thermostability of SMG1 [10]. Other lid modifications of lipase increased

Abbreviations: PVA, polyvinyl alcohol; OPA, oxidized PVA; OPH, OPA hydrolase; pNP, p-nitrophenyl; pNPA, pNP acetate; pNPB, pNP butyrate; pNPC, pNP caprylate; pNPL, pNP laurate; pNPP, pNP palmitate; DMSO, dimethyl sulfoxide; PEG, polyethylene glycol; DTT, dithiothreitol.

* Corresponding authors.
E-mail addresses: guo_rt@tib.cas.cn (R.-T. Guo), gcdu@jiangnan.edu.cn (G. Du).

[1] Y.Y. and T.P.K. contributed equally to this work.

http://dx.doi.org/10.1016/j.bbrc.2014.08.106
0006-291X/

the catalytic activity [11] and changed the substrate specificity and enantioselectivity [12].

The lid is the most variable region when the sOPH and pOPH structures are compared. The lid-mutant W255Y of pOPH showed the highest activity towards OPA but not pNP caprylate (pNPC). The mutants R264A and Y270F significantly improved catalytic efficiency towards both substrates, whereas the double mutant C257A/C267A showed decreased activity [4]. Trp255, located at the entrance of the active site tunnel, is essential for substrate specificity. In this study we measured the activity by using different chain-length pNP esters and compared the results of wild-type sOPH and pOPH as well as three pOPH mutants of the lid residue Trp255. The pNP esters were also used in complex crystallization, which however showed only the acid part as a hydrolyzed product. Possible roles of the lid disulfide bond were also investigated.

2. Materials and methods

2.1. Expression and purification of the wild-type and mutant enzymes

The wild-type sOPH and pOPH were expressed and purified as before, and so were the pOPH mutants of S172A, S172C, W255A, W255Y and W255F [4]. Here we also used hosts of *Escherichia coli* BL21 *trxB* (DE3) to produce the fusion proteins of pOPH with TEV cutting site and His-tagged thioredoxin in the vector pET32a. After 48 h cultivation in Luria-Bertani (LB) medium at 20 °C, the *E. coli* cells were collected by centrifugation at 7000×*g* and lysed with a French Press instrument in a buffer containing 25 mM Tris, pH 8.0, 150 mM NaCl, and 20 mM imidazole. After centrifugation at 17,000×*g* to remove cell debris, the supernatant containing pOPH was purified using a Ni–NTA column (GE Health, Uppsala, Sweden). The fusing protein was eluted and digested by TEV protease to remove the His-tagged thioredoxin. The untagged pOPH was eluted from a second Ni–NTA column, and further purified by using a Q column. Each purified protein was concentrated by a 60 mL Amicon Ultracentrifugal stirred cell with a 10,000 molecular weight cutoff membrane (Millipore, Bedford, MA, USA). The purity (>95%) was checked by using SDS–PAGE.

Construction of the sOPH mutant C241A/C248A used pET20b (+)-sOPH as the template with the forward primer 5′-GGTGAAAAA-GATCTGTGGGATGCTGGTCCACCTCTGGGTCTGGCTTCTGAT-TACCGTCCAACCACC-3′. After 72 h cultivation at 25 °C in Terrific Broth (TB) medium, the supernatant containing His-tagged sOPH was harvested by centrifugation at 7000×*g*, and loaded on a Ni–NTA column. The sOPH was eluted with about 60 mM imidazole in the above buffer and, after checking for purity, concentrated for activity test.

2.2. Analysis of enzymatic activity

OPH activity toward different pNP esters, including pNP acetate (pNPA; C2), pNP butyrate (pNPB; C4), pNPC (C8), pNPL (C12) and pNP palmitate (pNPP; C16), was analyzed in a reaction mixture (0.1% gum Arabic, 0.2% sodium deoxycholate and 50 mM Tris–HCl, pH 8.0) as previously described [4]. The increment of absorbance at 405 nm was recorded for 3 min at 37 °C. The kinetic parameters (K_m and k_{cat}/K_m) of sOPH, pOPH and its mutants were calculated by Michaelis–Menten curve fitting. Each value represents the mean of triplicate experiments by varying substrate concentrations (1.0 mM, 1.5 mM, 2.0 mM and 3.0 mM). The enzyme concentrations were determined by the Bradford method [13] using bovine serum albumin (BSA) as the standard.

2.3. Crystallization, data collection and structure determination

The wild-type (WT) pOPH was crystallized by using Crystal Screen II kit (Hampton Research, Laguna Niguel, CA) and sitting-drop method. The reservoir solution (No. 26) contained 30% PEG5000 MME, 0.1 M MES pH 6.5 and 0.2 M $(NH_4)_2SO_4$. No cryoprotectant was necessary for data collection of the WT crystal. The mutant pOPH crystals of S172A and S172C were obtained by using a reservoir solution of 0.1 M tri-sodium citrate, pH 5.6, 30% w/v PEG4000, and 0.3% w/v n-octyl-β-D-glucoside, similar to the previous conditions [4].

The complex crystals were prepared by soaking, in which a cryoprotectant solution (0.15 M tri-sodium citrate, pH 5.6, 35% w/v PEG4000, 0.8% w/v n-octyl-β-D-glucoside) was employed. To obtain pNPB and nonanedione complexes, the S172A and S172C crystals were soaked in the above cryoprotectant solution containing 20 mM pNPB and nonanedione (dissolved in DMSO), respectively, for at least 3 h before data collection. Later these crystals were found to contain butyrate and DMSO.

The X-ray diffraction datasets were collected at beam line BL13B1 and BL15A1 of the National Synchrotron Radiation Research Center (NSRRC, Hsinchu, Taiwan). The data were processed and scaled using the program HKL2000 [14]. Each asymmetric unit had one pOPH molecule. The structures were solved by molecular replacement, using PDB 3WL6 (chain A) as a search model. The models were refined by employing the programs CNS [15] and Coot [16]. PyMOL (DeLano Scientific, http://pymol.sourceforge.net/) was used in making figures.

2.4. PDB accession numbers

The coordinates of the pOPH crystals S172A/pNPB, S172C/DMSO, and WT/PEG have been deposited in the PDB with the accession codes of 3WWC, 3WWD, 3WWE, respectively.

3. Results

3.1. Characteristics of sOPH and pOPH with pNP esters as the substrates

As shown in Table 1, pOPH had lower K_m and higher k_{cat}/K_m values than sOPH for most pNP esters. The difference is most prominent in catalyzing the hydrolysis of the longer-chain substrates pNPC (C8) and pNPL (C12). It indicates that pOPH is endowed with the better catalytic properties in general. Moreover, the K_m values of both OPHs for pNP esters increased with the chain length of the fatty acyl substrates, whereas the k_{cat}/K_m values tended to decrease with the chain length, except for pNPB (C4). The k_{cat}/K_m for pNPB is significantly lower than those for all other substrates, no matter whether the enzyme is sOPH, pOPH or a lid mutant of Trp255.

To probe its function, Trp255 of pOPH was mutated to Ala, Tyr or Phe, making three separate mutants. All three mutants showed reduced catalytic activity for pNPA (C2). W255A and W255Y had improved k_{cat}/K_m values for pNPC (C8) and pNPL (C12). The activity of both mutants for pNPP (C16) was also enhanced, with a higher k_{cat}/K_m of W255A and a lower K_m of W255Y. The activity of W255F for pNPC, pNPL and pNPP all remained about the same as WT.

3.2. X-ray structures of pOPH complexes with butyrate, PEG and DMSO

Because pNPB showed significantly slower rate of hydrolysis than the other substrates, we tried to crystallize the OPH/pNPB complex. In the end a complex was obtained by soaking the pOPH mutant S172A crystal. Besides, the wild-type pOPH and the mutant

Table 1
Kinetic parameters of OPH for various pNP esters.

		sOPH WT	pOPH WT	pOPH W255A	pOPH W255Y	pOPH W255F
pNPA (C2)	K_m/mM	0.91 ± 0.03	0.71 ± 0.02	0.34 ± 0.02	0.83 ± 0.01	1.56 ± 0.03
	k_{cat}/s^{-1}	840 ± 20	560 ± 20	129 ± 6	150 ± 2	148 ± 3
	k_{cat}/K_m/s^{-1} mM^{-1}	919 ± 5	782 ± 2	380 ± 5	180 ± 1	95 ± 1
pNPB (C4)	K_m/mM	1.42 ± 0.04	0.83 ± 0.02	0.88 ± 0.04	1.02 ± 0.04	0.82 ± 0.03
	k_{cat}/s^{-1}	55 ± 2	47 ± 2	61 ± 3	112 ± 4	41 ± 2
	k_{cat}/K_m/s^{-1} mM^{-1}	39 ± 1	58 ± 2	70 ± 3	110 ± 1	49 ± 1
pNPC (C8)[a]	K_m/mM	2.2 ± 0.1	2.15 ± 0.07	2.6 ± 0.1	2.34 ± 0.09	1.9 ± 0.1
	k_{cat}/s^{-1}	390 ± 20	470 ± 20	600 ± 30	570 ± 30	400 ± 20
	k_{cat}/K_m/s^{-1} mM^{-1}	175 ± 10	216 ± 9	229 ± 1	250 ± 10	212 ± 5
pNPL (C12)	K_m/mM	5.9 ± 0.2	4.7 ± 0.2	3.7 ± 0.1	3.2 ± 0.1	4.7 ± 0.1
	k_{cat}/s^{-1}	270 ± 10	410 ± 10	600 ± 20	450 ± 20	500 ± 20
	k_{cat}/K_m/s^{-1} mM^{-1}	46 ± 2	89 ± 4	160 ± 7	143 ± 8	107 ± 3
pNPP (C16)	K_m/mM	8.5 ± 0.4	7.2 ± 0.2	6.0 ± 0.1	3.05 ± 0.09	5.6 ± 0.2
	k_{cat}/s^{-1}	145 ± 6	137 ± 3	330 ± 10	115 ± 3	140 ± 3
	k_{cat}/K_m/s^{-1} mM^{-1}	17.0 ± 0.1	19.0 ± 0.7	55 ± 1	38 ± 2	25 ± 2

[a] The kinetic data of pNPC have been presented previously [4].

S172C crystals were also obtained with bound PEG and DMSO molecules. All three crystals belong to the space group $P2_12_12_1$ and have similar unit-cell dimensions (Table 2). They are isomorphous to the previous crystals of S172C/ACA and S172A/PNPC (PDB 3WL7 and 3WL8) [4]. Despite the varied resolution of 1.5–2.1 Å, the protein structure remained the same, with root-mean-square deviations of 0.08–0.17 Å between the Cα atoms in these five structures.

Although the active-site Ser172 of pOPH had been mutated into alanine, the enzyme retained 20% activity [4]. As a result, the substrate was hydrolyzed and only butyrate was observed in the S172A/pNPB crystal. Interestingly, two molecules of butyric acid were found in the substrate binding cleft of pOPH, arranged in a "tail-to-tail" manner (Fig. 1A). The electron density clearly indicates the presence of two carboxyl "head" groups of butyric acid in the cleft (Fig. S1). These "heads" are bound in opposite directions and the hydrocarbon "tails" are approaching each other. With some disorder at the terminal methyl groups, the two butyric acids constitute a pimelate-like (C7) structure. The carboxylate group near catalytic triad of pOPH makes hydrogen bonds to Ser66, Tyr270 and His298, in a similar way as observed in the pOPH/caprylate complex [4]. The distal one also makes a hydrogen bond to Asn120 (Fig. 1B).

In the WT/PEG and S172C/DMSO crystals, both ligands bind to the same cleft where the previous ligands acetylacetone, caprylate and butyrate were located. This cleft is amphipathic in nature. It is only partially eclipsed by the lid and is open on the distal side to the bulk solvent, probably to facilitate binding to the natural long-chain substrate, OPA. There are two hydrogen bonds between the PEG fragment and the wild-type enzyme, but only one is formed between DMSO and the mutant (Fig. 1C).

Table 2
Data collection and refinement statistics of the pOPH complexes. Numbers in the parentheses are for the highest resolution shells.

	S172A/pNPB	S172C/DMSO	WT/PEG
Data collection			
Space group	$P2_12_12_1$	$P2_12_12_1$	$P2_12_12_1$
Unit cell *a*, *b*, *c* (Å)	58.3, 65.2, 84.3	58.5, 65.3, 84.2	58.4, 65.5, 84.4
α, β, γ (°)	90.0, 90.0, 90.0	90.0, 90.0, 90.0	90.0, 90.0, 90.0
Resolution (Å)	25–1.49 (1.54–1.49)	25–1.65 (1.71–1.65)	25–2.10 (2.18–2.10)
Unique reflections	52,709 (5167)	39,500 (3895)	19,106 (1656)
Average redundancy	4.5 (4.5)	6.0 (6.0)	6.1 (3.9)
Completeness (%)	99.8 (99.5)	100.0 (100.0)	97.6 (86.1)
Average $\langle I\rangle/\langle\sigma(I)\rangle$	24.6 (3.0)	23.6 (4.8)	25.5 (4.3)
R_{merge} (%)	5.8 (37.4)	8.3 (39.9)	7.8 (26.7)
Refinement			
No. of reflections	50,987 (4295)	38,410 (3610)	18,268 (1511)
R_{work} (95% data)	0.154 (0.232)	0.167 (0.208)	0.159 (0.271)
R_{free} (5% data)	0.173 (0.259)	0.193 (0.222)	0.208 (0.265)
RMSD bonds (Å)	0.017	0.0045	0.025
RMSD angles (°)	1.79	1.29	1.85
Ramachandran (%)			
Favored	96.7	96.7	97.3
Allowed	3.3	3.3	2.4
Outliers	0	0	0.3
$B_{average}$ ($Å^2$)/*atoms*			
Protein	14.4/2571	10.7/2580	23.2/2569
Ligands	28.8/25	19.7/17	36.7/9
Water	33.0/556	26.9/524	39.6/405
PDB code	3WWC	3WWD	3WWE

3.3. Effects of the lid cysteine modifications on sOPH and pOPH activity

The native crystal structures showed that two flanking cysteine residues in the lid region, Cys257/267 in pOPH and Cys241/248 in sOPH, are conserved despite the different lid lengths. They were supposed to form a disulfide bond, which was observed in the pOPH crystal. However, the equivalent disulfide bond was not seen in sOPH (Fig. 2A). In fact, the use of dithiotheritol (DTT) was required for crystallizing sOPH, but not for pOPH. To investigate the role of these two cysteine residues, we measured the activity of pOPH and sOPH in the presence and absence of DTT. As shown in Fig. 2B, the pOPH activity was reduced to about 10% by adding 5 mM DTT, while the sOPH activity was retained. We further constructed the double mutant C241A/C248A of sOPH. It exhibited the same activity level as did the wild-type sOPH (Fig. 2B). This is in contrast to the previous pOPH mutant C257A/C267A, which retained less than 20% activity [4].

4. Discussion

The lid region accounts for the major difference between pOPH and sOPH, and apparently the difference leads to the different characters in hydrolyzing pNP esters by these two enzymes. In addition to the overall length difference of the two lids, more detailed comparison and analysis would be required to explain the different catalytic property. In pOPH, the lid region is topped with a negatively charged amino acid (Asp261), followed by two positively charged amino acids (Arg259/264), whereas nonpolar

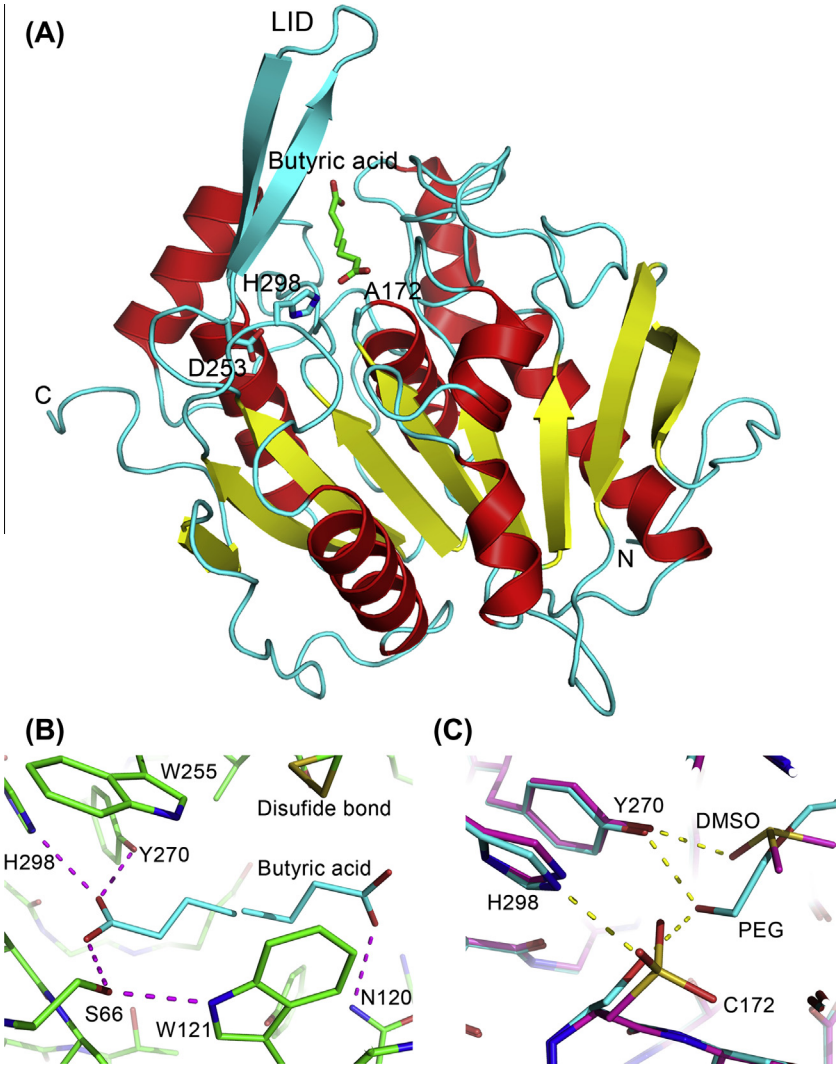

Fig. 1. The complexes of pOPH with butyric acid, PEG and DMSO. (A) In the S172A/pNPB crystal, only butyric acid was observed. The enzyme is shown as a ribbon diagram with red α-helices and yellow β-strands except for the lid, which is colored cyan as the loops. The ligand is bound with two different orientations, shown as green sticks. The catalytic triad is depicted as cyan sticks. (B) The butyric acid is hydrogen bonded to the protein side chains in either orientation. Here the amino acid residues are also shown as stick models. (C) The bound PEG in the WT crystal (cyan) and DMSO in the S172C mutant (pink) occupy the same place as the substrate. The hydrogen bonds in (B) and (C) are shown as dashed lines. (For interpretation of the references to color in this figure legend, the reader is referred to the web version of this article.)

amino acids are located at the base of the lid. The resulting surface is generally hydrophilic (Fig. 2C). By comparison, sOPH has a relatively short lid, which mainly contains nonpolar amino acids (Fig. 2D). The hydrophilic lid region of pOPH may account for its higher binding capacity and catalytic activity toward the pNP esters, which are polar compounds. The authentic substrate OPA contains multiple hydroxyl and ketone groups, and it is also a polar compound. Consequently, pOPH exhibited better binding capacity and catalytic activity than did sOPH for both pNP esters and OPA.

The bound butyric acid, as a hydrolysis product of pNPB, formed a tail-to-tail dimer in the active site cleft of pOPH, with two head groups hydrogen bonded to the side chains of Ser66, Asn120, Tyr270 and His298 (Fig. 1). Although the corresponding residues of Ser66 and Asn120 are both Thr in sOPH, the Thr side chains are still capable of hydrogen bond formations with butyric acid after proper rotations (Fig. S2). By occupying the active site cleft, butyric acid could be regarded as an inhibitor that hinders further pNPB binding to the active site of pOPH and sOPH, resulting in the low catalytic activity toward pNPB. The active site cleft is amphipathic in nature. DMSO and PEG also bind to the same cleft, and so does OPA. However, pNPA did not show a similar inhibiting effect. Perhaps the polar nature and high solubility of acetic acid in water prevents similar product inhibition as with butyric acid. The reduction of steric hindrance effect can be another reason. Although acetic acid could also form hydrogen bonds with the enzyme, the molecular size of acetic acid was not large enough to prevent other pNPA molecules from binding to the active site.

The catalytic triad in the active site tunnel is covered by the large side chain of Trp255 in pOPH (Trp239 in sOPH). Gao et al. found a similar Trp residue covering the entrance of the active site of a lipase from *M. globosa* [10]. Mutating that Trp to Leu or Phe changed substrate preference of the lipase. Here we mutated Trp255 of pOPH into Ala, Phe or Tyr, and all three mutants showed reduced k_{cat}/K_m values for the short-chain pNPA, suggesting the importance of Trp255 in sequestering the active site from the solvent and binding the substrate in a productive mode. With the longer acyl chains in pNPC, pNPL and pNPP, probably the nonpolar nature of the substrate can exclude solvent from the active site, and the smaller side chains of Ala and the amphipathic Tyr can facilitate product release. Consequently the k_{cat}/K_m values of W255A and W255Y were higher.

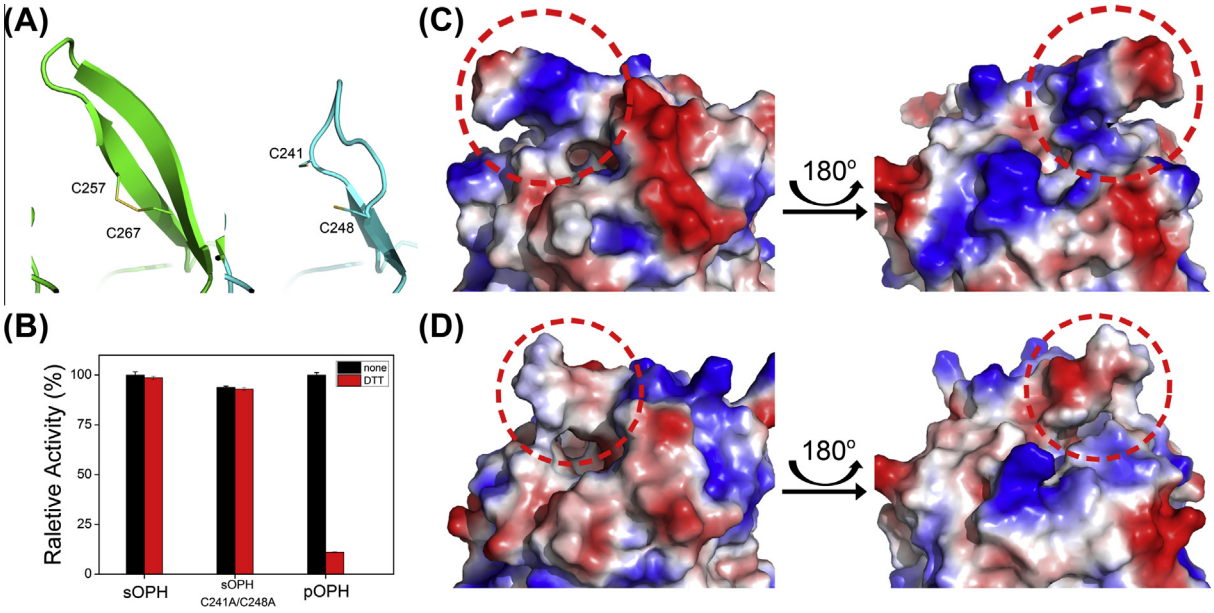

Fig. 2. Structural difference of the lid region. (A) On the left side the two lid residues Cys257/267 formed a disulfide bond in the pOPH crystal (green). On the right the equivalent Cys241/248 in sOPH (cyan) did not show a similar bond. (B) By using pNPA as the substrate, little effect of DTT on the sOPH activity was observed. The double mutant C241A/C248A of sOPH remained active. In contrast, DTT reduced the activity of pOPH (red bar at the right). (C) The surface of pOPH is viewed in two opposite directions. (D) That of sOPH is shown in two equivalent orientations as in (C). The surfaces are colored according to electrostatic potential, with blue and red representing positive and negative charges. The lid region is shown by using red circle. (For interpretation of the references to color in this figure legend, the reader is referred to the web version of this article.)

As a strong reducing agent, DTT could effectively prevent formation of unwanted polymer caused by incorrect inter-molecular disulfide bonds in a protein sample during crystallization. To obtain high-quality crystals of sOPH, 5 mM DTT was included in the protein sample. Therefore, C241/248 in sOPH did not form a disulfide bond in the crystal structure (Fig. 2A). Three disulfide bonds formed by the other Cys pairs were nevertheless observed, probably because they were not exposed to the solvent. Meanwhile, no DTT was needed in crystallizing pOPH, and C257/267 formed the fourth disulfide bond. The reduced activity of pOPH by adding DTT (Fig. 2B) and by making the mutant C257A/C267A [4] suggests the importance of this disulfide bond, which was supposed to be present in sOPH under non-reducing conditions. However, little DTT effect was observed with sOPH, and the activity was also retained in the mutant C241A/C248A.

Although the polyhydroxybutyrate deploymerase (PHB) from *Penicillium funiculosum* [17] does not show a lid-like structure, several PHB related enzymes, found by BLAST, contain an equivalent lid region (Fig. S3). The lids vary in length but two conserved Cys residues are found in those with the same length as in pOPH. Presumably a disulfide bond is formed there. The mammalian lipase I (LIPI) has a short lid region covering the active site, and two cysteine residues are located on the N and C terminal sides of the lid region, also forming a disulfide bond [18]. Because of their location on the cell membrane [2] or in the periplasm [1], both pOPH and sOPH are likely to form the lid disulfide under natural conditions. Apparently these results indicate that the disulfide bond of C257/267 in pOPH maintains the stability of lid regions, which play a key role in catalysis. In contrast, the two Cys residues C241/248 in sOPH are dispensable. One possibility is that the longer amphipathic lid of pOPH needs a stabilizing disulfide bond, but the shorter lid of sOPH does not.

In this study we found the three mutants W255A, W255Y and W255F of pOPH all retained considerable activity, especially for the pNP ester substrates with longer acyl chains. This is somewhat different from the previous observations by using OPA as the substrate [4]. For OPA, W255A and W255F showed reduced activity but W255Y showed enhanced activity. The discrepancy may be a result of the globally amphipathic nature of OPA, in contrast to a mixture of the polar and nonpolar moieties in the pNP esters. The medium chain-length substrates of pNPC (C8) and pNPL (C12) seemed to work better than the others. They did not show product inhibition as did pNPB (C4), and thus could be better candidates for optimized artificial substrates in preliminary activity screening.

Acknowledgments

This work was supported by Program for Changjiang Scholars and Innovative Research Team in University (No. IRT1135), the National High Technology Research and Development Program of China (863 Program, 2012AA022202), the Priority Academic Program Development of Jiangsu Higher Education Institutions, the 111 Project (111-2-06). We thank the National Synchrotron Radiation Research Center of Taiwan for beam-time allocation and data-collection assistance.

Appendix A. Supplementary data

Supplementary data associated with this article can be found, in the online version, at http://dx.doi.org/10.1016/j.bbrc.2014.08.106.

References

[1] W. Klomklang, A. Tani, K. Kimbara, R. Mamoto, T. Ueda, M. Shimao, F. Kawai, Biochemical and molecular characterization of a periplasmic hydrolase for oxidized polyvinyl alcohol from *Sphingomonas* sp. strain 113P3, Microbiology 151 (2005) 1255–1262.
[2] M. Shimao, T. Tamogami, S. Kishida, S. Harayama, The gene *pvaB* encodes oxidized polyvinyl alcohol hydrolase of *Pseudomonas* sp. strain VM15C and forms an operon with the polyvinyl alcohol dehydrogenase gene *pvaA*, Microbiology 146 (2000) 649–657.
[3] F. Kawai, X.P. Hu, Biochemistry of microbial polyvinyl alcohol degradation, Appl. Microbiol. Biotechnol. 84 (2009) 227–237.
[4] Y. Yang, T.-P. Ko, L. Liu, J. Li, C.-H. Huang, H.-C. Chan, F. Ren, D. Jia, A.H.-J. Wang, R.-T. Guo, J. Chen, G. Du, Structural insights into enzymatic degradation of

oxidized polyvinyl alcohol, ChemBioChem (2014), http://dx.doi.org/10.1002/cbic.201402166.
[5] M. Holmquist, Alpha beta-hydrolase fold enzymes structures, functions and mechanisms, Curr. Protein Pept. Sci. 1 (2000) 209–235.
[6] M. Nardini, B.W. Dijkstra, α/β Hydrolase fold enzymes: the family keeps growing, Curr. Opin. Struct. Biol. 9 (1999) 732–737.
[7] C.K.-M. Chen, G.-C. Lee, T.-P. Ko, R.-T. Guo, L.-M. Huang, H.-J. Liu, Y.-F. Ho, J.-F. Shaw, A.H.-J. Wang, Structure of the alkalohyperthermophilic *Archaeoglobus fulgidus* lipase contains a unique C-terminal domain essential for long-chain substrate binding, J. Mol. Biol. 390 (2009) 672–685.
[8] G. Santarossa, P.G. Lafranconi, C. Alquati, L. DeGioia, L. Alberghina, P. Fantucci, M. Lotti, Mutations in the "lid" region affect chain length specificity and thermostability of a *Pseudomonas fragi* lipase, FEBS Lett. 579 (2005) 2383–2386.
[9] T. Xu, L. Liu, S. Hou, J. Xu, B. Yang, Y. Wang, J. Liu, Crystal structure of a mono- and diacylglycerol lipase from *Malassezia globosa* reveals a novel lid conformation and insights into the substrate specificity, J. Struct. Biol. 178 (2012) 363–369.
[10] C. Gao, D. Lan, L. Liu, H. Zhang, B. Yang, Y. Wang, Site-directed mutagenesis studies of the aromatic residues at the active site of a lipase from *Malassezia globosa*, Biochimie 102 (2014) 29–36.
[11] X.-W. Yu, S.-S. Zhu, R. Xiao, Y. Xu, Conversion of a *Rhizopus chinensis* lipase into an esterase by lid swapping, J. Lipid Res. 55 (2014) 1044–1051.
[12] F. Secundo, G. Carrea, C. Tarabiono, P. Gatti-Lafranconi, S. Brocca, M. Lotti, K.-E. Jaeger, M. Puls, T. Eggert, The lid is a structural and functional determinant of lipase activity and selectivity, J. Mol. Catal. B 39 (2006) 166–170.
[13] M.M. Bradford, A rapid and sensitive method for the quantitation of microgram quantities of protein utilizing the principle of protein-dye binding, Anal. Biochem. 72 (1976) 248–254.
[14] Z. Otwinowski, W. Minor, Processing of X-ray diffraction data, Methods Enzymol. 276 (1997) 307–326.
[15] A.T. Brunger, P.D. Adams, G.M. Clore, W.L. DeLano, P. Gros, R.W. Grosse-Kunstleve, J.-S. Jiang, J. Kuszewski, M. Nilges, N.S. Pannu, Crystallography & NMR system: a new software suite for macromolecular structure determination, Acta Crystallogr. D 54 (1998) 905–921.
[16] P. Emsley, K. Cowtan, Coot: model-building tools for molecular graphics, Acta Crystallogr. D 60 (2004) 2126–2132.
[17] T. Hisano, K.-I. Kasuya, Y. Tezuka, N. Ishii, T. Kobayashi, M. Shiraki, E. Oroudjev, H. Hansma, T. Iwata, Y. Doi, The crystal structure of polyhydroxybutyrate depolymerase from *Penicillium funiculosum* provides insights into the recognition and degradation of biopolyesters, J. Mol. Biol. 356 (2006) 993–1004.
[18] Roger S. Holmes, Laura A. Cox, Review comparative structures and evolution of mammalian lipase I (LIPI) genes and proteins: a close relative of vertebrate phospholipase LIPH, Nat. Sci. 4 (2012) 1165–1178.